BULGARIAN ACADEMY OF SCIENCES

CYBERNETICS AND INFORMATION TECHNOLOGIES • Volume **24**, No 1
Sofia • 2024 Print ISSN: 1311-9702; Online ISSN: 1314-4081
DOI: 10.2478/cait-2024-0008

Degradation Recoloring Deutan CVD Image from Block SVD Watermark

Zoran N. Milivojević[1], *Bojan Prlinčević*[2], *Milan Cekić*[3], *Dijana Kostić*[1]

[1]*Academy of Applied Technical and Preschool Studies, Niš, Serbia*
[2]*Kosovo and Metohija Academy of Appl. Studies, Leposavić, Serbia*
[3]*Mikkelsen Electronics, Niš, Serbia*
E-mails: zoran.milivojevic@akademijanis.edu.rs bojan.prlincevic@akademijakm.edu.rs mce@mi-ec.com dijanaaricija79@gmail.com

***Abstract*:** *People with Color Vision Deficiency* (*CVD*), *which arises as a deformation of the M cones in the eye, cannot detect the color green in the image* (*deutan anomaly*). *In the first part of the paper, deutan anomalous is described. After that, the image recoloring algorithm, which enables Deutan CVD people to see a wider spectrum in images, is described. Then, the effect of the Recoloring algorithm on images with inserted watermark is analyzed. An experiment has been carried out , in which the effect of the Recoloring algorithm on the quality of extracted watermark and Recoloring image is studied. In addition, the robustness of the inserted watermark in relation to spatial transformations* (*rotation, scaling*) *and compression algorithms has been tested. By applying objective measures and visual inspection of the quality of extracted watermark and recoloring image, the optimal insertion factor* α *is determined. All results are presented in the form of pictures, tables and graphics.*

***Keywords*:** *Trichromacy, Deutanomaly, Image recoloring, Digital image watermark, SVD Algorithm.*

1. Introduction

The first part of the Human Visual System (HSV) is the eye. Through the optics of the eye, the spatial distribution of the light from the environment is projected onto the retina. In this way, a two-dimensional image on the retina is formed. The retina is covered with photoreceptors, that is, light-sensitive nerve cells [1]. The photoreceptors are sensitive to light in the wavelength range λ is 370-720 nm. After the nerve cells are activated by the light, a series of chemical and electrical impulses are triggered. The impulses are sent through the fiber of the optic nerve to the various parts of the brain. In the brain, the received impulses are processed, and, based on this, visual perception is created. The retina has two types of photoreceptors, which, according to their shape, are named: a) rods, and b) cones [2]. The retina has up to 120 million rods. The rods are active at the lower light intensities. The rods realize so-called black and white vision, as well as night vision. The retina has up to 6 million

cones. The cones are active at higher light intensities. The cones realize color vision. Humans have three different types of the cones, which are sensitive to the visible light, in the range of the wavelengths: a) Long, L, b) Medium, M, and c) Short, S. An eye with this type of cone (L, M and S) realizes normal, i.e., trichromatic vision. People with trichromatic vision can see all colors in the wavelength range of λ is 370-720 nm. People with Color Vision Deficiency (CVD) have a problem with distinguishing some, or, in more severe forms of CVD, all colors [3].

CVD can be classified as anomalous type: a) trichromacy (some types of the cones do not function in their visual range, but are shifted to one frequency side), b) dichromacy (with this anomaly there are only two types of the cones, which are capable of perceiving color [4]. The functions of the third type of the cones are completely inactive) and c) monochromacy (none of the cones are active. Only the rods are active and enable black-and-white vision) [5]. Digital image processing includes, among other things, pixel intensity processing. In a color image, each pixel is composed of a Red (R), Green (G) and Blue (B) component. Grassmann's laws describe empirical results, based on which it is concluded that the resulting color is obtained by linearly mixing two or more colors. Based on that, it is possible to represent the primary colors R, G and B with vectors, and associate them with Cartesian coordinates of three-dimensional space. In this way, the RGB color space, in which the colors in the space are represented by vectors, and the laws of vector algebra can be applied, is defined. People have three types of cones for color detection (L, M and S), and, in order to apply vector algebra when calculating the color experience, it is possible to form the LMS color space. By applying the analysis of the color in the RGB or LMS color space, it is possible, among others, to perform geometric interpretation of the results and perform their analysis, spatial transformations such as rotation, color scaling, etc. In order to help CVD people to be able to see a wider range of colors, it is necessary to perform processing of the image [6] by color analysis in one of the color spaces (RGB, LMS, ...). Analyzed from a geometrical aspect, by applying image processing, it leads to a spatial shift of the color position in the color space. The spatial displacement of the colors is such that the distance between all colors increases. Visual analysis shows that there are color changes in the image, such that CVD people have a better visual experience. Image processing for CVD people, which is based on changing the location of colors in the LMS color space, in the scientific literature is called Recoloring RC image [7]. A large number of the Recoloring algorithms have been described [8-12]. Recoloring algorithms could be implemented in computer monitors, mobile phones, etc. The intensity of the effect of Recoloring algorithms could be adjusted for the individual user, depending on the degree of CVD. In addition, various web sites could allow users to use images and videos for CVD people. Image and video designers could, even in the creation phase, by using Recoloring algorithms on their systems, determine how their image or video will be visible to the CVD people. In general, the implementation of Recoloring algorithms can be implemented using specialized hardware or software, depending on the specified speed of realization (real-time).

Intensive exchange of the images over the Internet enables unauthorized use of the images. For this reason, a need arose to protect the RC image from unauthorized

use. One of the ways of copyright protection is to insert watermarks into the image. The watermark can be: a) visible, and b) invisible. The visible watermark clearly indicates the owner of the image. However, the visible watermark degrades the quality of the image, especially in the part of the image where it is inserted (typical marking of TV channels). The invisible watermark can be inserted into the image in: a) spatial, and b) transformation domain. The insertion of an invisible watermark is realized with the insertion factor, so that the watermark: a) does not cause visible degradation of the RC image, and b) is robust, that is, after extraction from the image, it is of sufficient quality to prove copyright. The paper [13] describes an algorithm for inserting and extracting watermarks from RC images, which has been created for Protan CVD people. Protan CVD is an anomaly of the L cones such that their spectral sensitivity is shifted in the direction of the spectral sensitivity of the M cones. In order to insert the watermarks, using the Block SVD (Singular Value Decomposition) algorithm, the RC image processing is realized in the LMS color space [14, 15].

In this paper, the effect of the Deutan RC algorithm on the inserted watermark is analyzed. First, the Deutan CVD anomaly is described. Deutan CVD people, partially, or even completely, cannot see the color green in the image. After that, the Deutan RC Algorithm is described. The RC Algorithm is used to move the color position in the LMS space [15]. Therefore, the generated RC image is colorimetrically different from the original image. However, the generated RC image allows Deutan CVD people to be able to perceive green objects in the image, but with colorimetric inaccuracy. After that, the modified Block SVD watermarking [16] is described. The modification has been made by the authors of this paper. In the second part of this paper, an experiment is described. The following items have been analyzed in the experiment: a) impact of the RC Algorithm on the quality of the extracted watermark, b) the influence of the watermark on the visual quality of the RC image, and c) testing the robustness of the inserted watermark in relation to spatial transformations (rotation, scaling) and compression algorithms (JPEG, TIFF, PGN and HDF). The Deutan RC Algorithm has been applied to Test images from the Test database created for the purposes of the Experiment. The Test base is composed of 10 images from BSDS500 (Berkeley Segmentation Dataset) [17]. The algorithm, according to which the experiment has been carried out, is presented. The inserted Watermark is the *Logo* of Academy of Applied Technical and Preschool Studies, Niš, Serbia. The performance of extracted watermark and RC image has been tested using: a) objective measures, and b) subjective measures (visual inspection of the quality of RC images and watermarks). As objective measures, measures that are intensively used in digital image processing: a) Mean Square Error, MSE, b) Peak Signal to Noise Ratio, PSNR, c) Normalized Correlation, NC, and d) Structure Similarity Index, SSIM, have been used. The subjective analysis has been carried out by the Test Group. The Test group has been composed of third-year students of the Department for Information and Communication Technologies (Academy of Applied Technical and Preschool Studies, Niš, Serbia). Objective measures are determined for various values of the watermark insertion factor α. Through the comparative analysis of the results, the conclusion about the effect of the watermark on the RC image, is derived. The critical value of the watermark insertion factor α is determined using the visual

inspection of the RC image. The results are presented graphically. In addition, Test images, RC images and watermarks are shown.

Further organization of work is as follows. In Section 2, Deutan CVD anomalous is presented. In Section 3, the Recoloring algorithm for Deutan CVD anomaly is presented. In Section 4, the Watermarking algorithm, is described. In Section 5 the experiment is described. Section 6 is the Conclusion.

2. Deutan CVD anomaly

The normalized spectral sensitivity of the human cone of the short $S(\lambda)$, middle $M(\lambda)$ and long $L(\lambda)$ wavelength types, for normal, i.e., trichromatic vision, are shown in Fig. 1a. In Fig. 1b is shown a Test image with a wide range of the colors, as seen by a people with normal vision.

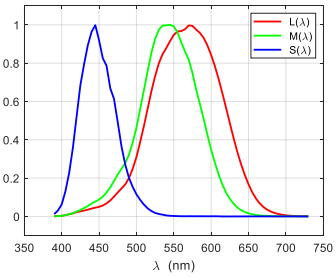

(a)

(b)

Fig. 1. Normal vision: (a) normalized spectral sensitivity of human cone cells of short $S(\lambda)$, middle $M(\lambda)$, long $L(\lambda)$ wavelength, (b) visual perception of the Test image [21]

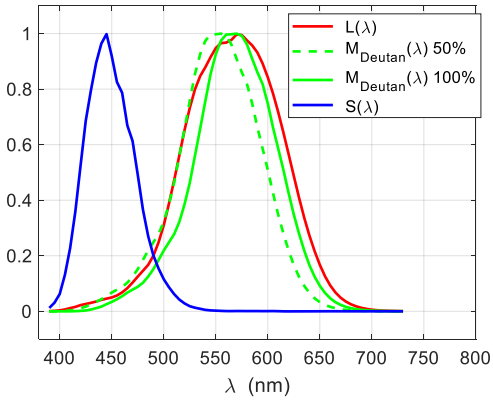

(a)

(b)

(c)

Fig. 2. Deutan CVD: normalized spectral sensitivity of the cones for Deutan CVD (50% and 100%), and Test images as seen by a people (a), with 50% Deutan CVD (b), and with 100% Deutan CVD (c)

In CVD people, some, or all types of the cone, do not function correctly. The deuteranomaly (deuteranopia), i.e., Deutan CVD, occurs as a consequence of the deformation of the M cones. The deformation is manifested as a shift of the amplitude characteristic of light sensitivity of the M cones by $\Delta\lambda$ in the direction of the L range. Therefore, the light energy from the red color range is represented as green color in

the M channel. The Deutan CVD effect increases with increasing $\Delta\lambda$ [20]. Fig. 2a shows the normalized amplitude characteristics for 50% ($\Delta\lambda$ = 10 nm) and 100% Deutan CVD ($\Delta\lambda$ = 20 nm). The visual color experience of the Test image (Fig. 1a) in people with 50% Deutan CVD, is shown in Fig. 2b. The visual color experience for 100% Deutan CVD is shown in Fig. 2c. It is clearly seen that the Deutan CVD people cannot see a wide range of colors. Deutan CVD people often cannot see all the color details in the image (Fig. 2b and Fig. 2c). In order to reduce this discomfort, it is possible to perform color correction (recoloring) in the image so that people with Deutan CVD problem can see better. Image recoloring is the creation of a different version of the image colors that is more suitable for Deutan CVD people.

3. Recoloring algorithm for Deutan CVD anomaly

In paper [15] an RC image recoloring algorithm for CVD people is described. In this Section, the Modified RC algorithm from [15], which is intended for recoloring images for Deutan CVD people [19], is described. Recoloring is realized by transforming colors from the RGB into the LMS color space. The Deutan CVD RC Algorithm is implemented in six steps as follows.

Deutan CVD RC Algorithm

Input: Image *I*

Output: RC image *Y*

Step 1. Transform from the RGB color space (I_{RGB}) to the LMS color space (I_{LMS}):

$$\begin{bmatrix} L \\ M \\ S \end{bmatrix} = \begin{bmatrix} 17.8824 & 43.5161 & 4.11935 \\ 3.45565 & 27.1554 & 3.86714 \\ 0.0299566 & 0.184309 & 1.46709 \end{bmatrix} \times \begin{bmatrix} R \\ G \\ B \end{bmatrix}, \tag{1}$$

where R, G, and B are the red, green, and blue color components of image *I* in the RGB color space.

Step 2. Simulated color experience at the Deutan CVD people:

$$\begin{bmatrix} L_p \\ M_p \\ S_p \end{bmatrix} = \begin{bmatrix} 1 & 0 & 0 \\ 0.4942 & 0 & 1.2483 \\ 0 & 0 & 1 \end{bmatrix} \times \begin{bmatrix} L \\ M \\ S \end{bmatrix}, \tag{2}$$

where L_p, M_p and S_p are the color components in the LMS color space.

Step 3. Error between normal and color blind (CB) perception in the LMS space:

$$\begin{bmatrix} E_L \\ E_M \\ E_S \end{bmatrix} = \begin{bmatrix} L \\ M \\ S \end{bmatrix} - \begin{bmatrix} L_p \\ M_p \\ S_p \end{bmatrix}. \tag{3}$$

Step 4. Distribution of the error to *M* and *S* color components:

$$\begin{bmatrix} E_{L\_MOD} \\ E_{M\_MOD} \\ E_{S\_MOD} \end{bmatrix} = \phi \begin{bmatrix} 1 & 0.1 & 0 \\ 0 & -0.2 & 0 \\ 0 & 0.1 & 1 \end{bmatrix} \times \begin{bmatrix} E_L \\ E_M \\ E_S \end{bmatrix}, \tag{4}$$

where ϕ is a scalar between 0 and 1.

Step 5. Recolored image in LMS space (RC image):

$$\begin{bmatrix} L_{p,RE} \\ M_{p,RE} \\ S_{p,RE} \end{bmatrix} = \begin{bmatrix} E_{L\_MOD} \\ E_{M\_MOD} \\ E_{S\_MOD} \end{bmatrix} + \begin{bmatrix} L \\ M \\ S \end{bmatrix}. \tag{5}$$

Step 6. Recolored image in RGB space:

$$\begin{bmatrix} R_{re} \\ G_{re} \\ B_{re} \end{bmatrix} = \begin{bmatrix} 0.080944 & -0.130504 & 0.11672 \\ -0.01025 & 0.054019 & -0.11362 \\ -0.00037 & -0.004122 & 0.69351 \end{bmatrix} + \begin{bmatrix} L_{p,RE} \\ M_{p,RE} \\ S_{p,RE} \end{bmatrix}, \tag{6}$$

where R_{re}, G_{re}, and B_{re} are the recolored color components in the RGB color space.

As an example of the application of the previously described RC Algorithm over the Test image, the CB and RC images are generated. The Test image is shown in Fig. 3a. The Deutan CVD people experience colors as in Fig. 3b (CB image, Step 2). After color transformation by the RC Algorithm, the RC image (Fig. 2c), which is suitable for Deutan CVD people, is generated.

a) b) c)

Fig. 3. Test image [22] (a), CB image (b), and RC image (c)

4. Block SVD Watermarking Algorithm

The Block SVD Watermarking Algorithm is presented in [16]. Binary images, whose pixel intensities have only two values (0 or 1, or 0 and 255), are used as watermarks with the Block SVD Watermarking algorithm. In order to insert some data (e.g., a hash, a text file, an ID number, etc.), with the Block SVD Watermarking algorithm, it is necessary to create a binary image (watermark) in which the desired data is inserted. The reason for forming a watermark in the form of a binary image of dimensions $(M/4) \times (N/4)$, where $M \times N$ are the dimensions of the image in which the watermark should be inserted, lies in the fact that in the image, in the spatial domain, in each block (4×4 pixels), the spatially appropriate pixel of the watermark should be inserted. The process of inserting one pixel of the watermark into one 4×4 image block involves analyzing of the intensity of pixels in the transformation domain. For this purpose, Singular Value Decomposition (SVD) is performed over block **X**. The result of applying SVD is the decomposition $\mathbf{X} = \mathbf{U.S.V}^T$, where **U** (left singular vector) and **V** (right singular vector) are orthogonal matrices. **S** is a diagonal matrix, $\mathbf{S} = \text{diag}(\sigma_1, \sigma_2, \sigma_3, \sigma_4)$, whose elements are singular values, and satisfying $\sigma_1 \geq \sigma_2 \geq \sigma_3 \geq \sigma_4$. The idea of inserting one pixel of the watermark is based on the analysis relations between σ_2 and σ_3. In the case that $\sigma_2 > \sigma_3$, then a correction is made, so that $\sigma_2 = \sigma_3$. After that, the σ_2 correction is performed by inserting the value of the corresponding pixel w of the watermark, that is, $\sigma_2 = \sigma_2 + \alpha\, w$, where α is the insertion

factor of the watermark. For the case that $w = 1$, there is a change of the singular value σ_2, which therefore becomes greater than σ_3. In order to preserve the regularity of the SVD transformation, that is to ensure that $\sigma_1 \geq \sigma_2$, in case it is not, the correction $\sigma_1 = \sigma_2$ is made. In this way, one bit of the watermark, by applying transformation, i.e., decomposition, is scattered spatially over the entire 4×4 block. The invisibility of the watermark in the image, that is, more precisely, the absence of visual degradation of the image, is achieved by selecting the insertion factor α. Determining the parameter α comes down to a compromise between the quality of the image (less α) and the quality of the watermark (greater α), that is, it comes down to determining the maximum α, in which the visual quality of the image is not impaired. In this paper, embedding of the watermark is done in a color image. Embedding of the watermark is done in the *M* component of the image in the LMS color space.

Watermark Embedding Algorithm

Input: I – image in the RGB color space. W – watermark ($M_{\text{wm}} \times N_{\text{wm}}$). Insertion factor α.

Output: I_{wm} – watermarked image.

Step 1. Transformation of image I from RGB color space (I_{RGB}) to LMS color space (I_{LMS}).

Step 2. Extracting the M component from the image I_{LMS}.

Step 3. The image component M is divided into non-overlapping blocks $B_{i,j}$, dimension 4 × 4, where $i = 1, \ldots, M_{\text{wm}}$, and $j = 1, \ldots, N_{\text{wm}}$.

Step 4. SVD transformation is performed over each block $B_{i,j}$, of the M image component: $B_{i,j} = U_{i,j} \cdot S_{i,j} \cdot V^{\text{T}}_{i,j}$, where $U_{i,j}$ and $V_{i,j}$ are orthogonal matrices, $S_{i,j}$ is a diagonal matrix $S_{i,j} = \text{diag}(\sigma_1, \sigma_2, \sigma_3, \sigma_4)$.

Step 5. Assigning the value $\sigma_{3n} = \sigma_2$.

Step 6. Inserting the bit $W_{i,j}$ of the watermark W: $\sigma_{2n} = \sigma_2 + \alpha \cdot W_{i,j}$.

Step 7. Modification of the matrix S according to: **IF** $\sigma_1 < \sigma_{2n}$ **THEN** $\sigma_{1n} = \sigma_{2n}$; **ELSE** $\sigma_{1n} = \sigma_1$; **END**, after which the diagonal matrix with watermark bit is $S_{i,j} = \text{diag}(\sigma_{1n}, \sigma_{2n}, \sigma_{3n}, \sigma_4)$.

Step 8. Reconstruction of the block with the watermark $B_{W_{i,j}}$: $B\,B_{W_{i,j}} = U_{i,j} \cdot S\,B_{W_{i,j}} \cdot V^{\text{T}}_{i,j}$.

Step 9. Reconstructing the M_{wm} component with the embed watermark $M_{\text{wm}} \Leftarrow B_{W_{i,j}}$.

Step 10. The reconstructed image with the watermark ($I_{W_{\text{LMS}}}$) is translated from the LMS color space into the RGB color space ($I_{W_{\text{RGB}}}$), and the image with the embedded watermark I_{wm} is finally obtained.

Watermark Extraction Algorithm

Input: I_{wm} – Image with watermark. $M_{\text{wm}} \times N_{\text{wm}}$ – dimensions of watermark block.

α – insertion factor.

Output: W_{e} – extracted watermark.

Step 1. Transformation of image I_{wm} from RGB color space ($I_{W_{\text{RGB}}}$) to LMS color space ($I_{W_{\text{LMS}}}$).

Step 2. Extracting the M_w component from the image $I_{W_{LMS}}$.

Step 3. The image component M_W is divided into non-overlapping blocks B_W, dimension 4 × 4, where $i = 1, ..., M_{wm}$ and $j = 1, ... , N_{wm}$.

Step 4. SVD transformation is performed over each block $B_{W_{i,j}}$, of the M_W image component: $B_{W_{i,j}} = U_{i,j} \cdot S_{W_{i,j}} \cdot V^T_{i,j}$.

Step 5. The values of the watermark bit, $W_{e_{i,j}}$, which is extracted from the block $B_{W_{i,j}}$ are determined according to **IF** $\sigma_2 < \sigma_3$; **THEN** $W_{e_{i,j}} = 1$; **ELSE** $W_{e_{i,j}} = 0$; **END**.

5. Experimental results and result analysis

5.1. Experiment

An experiment in which the recoloring of the Test images: a) with and b) without an inserted watermark, has been performed. Recoloring Test image for the Deutan CVD people, using the algorithm described in Section 3, is performed. The watermark is inserted using the Block SVD Algorithm, which is described in Section 4. Watermark insertion has been done by processing the Test image in LMS color space. With the recoloring process, the *M* color component is the least affected component [13]. In accordance with this fact, the insertion of the watermark has been realized in the *M* component of the Test image. The aim of the experiment is to determine the influence of the inserted watermark on the quality of the RC image. In addition, the quality of the extracted watermark from the RC image has been analyzed. Analyzes have been performed for different values of the insertion factor α. In the second part of the experiment, the robustness of the inserted watermark has been tested. In order to test the robustness, some attacks on the RC image have been performed. The attacks have been implemented: a) in the spatial domain (scaling, rotation), and b) using compression algorithms (JPEG, TIFF, PGN and HDF). The rotation is performed for the angle $\theta = \{15^o, 30^o, 45^o, 60^o, 75^o\}$. Scaling has been done for the scaling factor $S_f = \{0.9, 0.8, 0.7, 0.6, 0.5\}$. JPEG compression has been performed for visual quality Q_{JPG} = {100%, 90%, 80%, 70%, 60% and 50%}. By testing the quality of the extracted watermark, the robustness assessment has been performed. The results of the experiment (RC image, extracted watermark) have been analyzed using: a) objective measures, and b) subjective measure (visual inspection of images). The quality of the RC image and extracted watermark has been analyzed using standard objective measures, which are intensively used in digital signal processing, especially in digital image processing: a), MSE, b), PSNR, c) NC, and SSIM. Objective measures between the corresponding Test images with watermarks in relation to the Test images without watermarks have been calculated. In the same way, the objective measures between the inserted watermark and extracted watermarks have been determined. Visual inspection has been done by the Test Group. The Test group was composed of third-year students from the Department of Information and Communication Technologies (Academy of Applied Technical and Preschool Studies, Niš, Serbia). 30 students participated, with an average age of 21.45 years, and a gender structure of 15 males and 15 females. The subjective analysis has been realized by visual inspection of the quality of the RC image in which the watermark is embedded. In this way, the critical value of the insertion factor α_c has been

determined. The critical value of the insertion factor α_c is the one at which visual quality degradation of the Test image occurs due to the inserted watermark. In addition, an analysis of the visual quality of the extracted watermark has been performed. The extracted watermark should satisfy the visual qualities to be valid for proving the ownership of the image. The results of the experiment are presented in the form of RC images, watermark images, tables and graphics. The experiment was done in in five steps as follows.

Experimental Algorithm

Input: I – Test image in the RGB color space. W – binary watermark. Insertion factor α.

Output: Objective measures MSE, PSNR, NC and SSIM.

Step 1. Inserting a watermark W into Test image I with the insertion factor α, and creating an image with a watermark I_{wm}.

Step 2. Changing the colors of the image I_{wm} by applying the RC Algorithm, RC image with changed colors, which are adapted to Deutan CVD people, are created.

Step 3. Extracting watermark W_e from RC image.

Step 4. Visual inspection of the RC image and determination of α_c at which the watermark begins to be seen in the image.

Step 5. Determining the performance of the extracted watermark W_e and RC image using MSE, PSNR, NC and SSIM measures.

5.2. Base

For the experiment purposes the Image Base has been created. The Image Base is made up of: a) 10 images from BSDS500 (Berkeley Segmentation Dataset) [17], and b) an electronic watermark. The Test images are shown in Fig. 3: I1 (Fig. 3a), I2 (Fig. 3b), I3 (Fig. 3c), I4 (Fig. 3d), I5 (Fig. 3e), I6 (Fig. 3f), I7 (Fig. 3g), I8 (Fig. 3h), I9 (Fig. 3i), and I10 (Fig. 3j). The Logo of the Academy of Applied Technical and Preschool Studies, Niš, Serbia, 32 × 32 pixels, has been used as a watermark. In order to distribute the watermark over the entire Test images, a new watermark (90 × 180 pixels), which has been obtained from multiple repetitions of the Logo (Fig. 6a), was created.

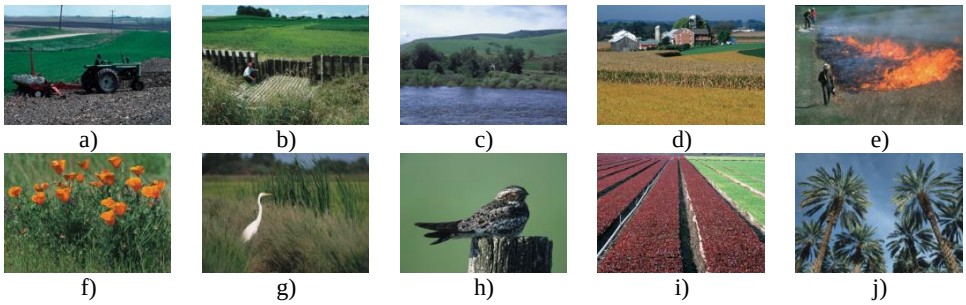

Fig. 3. Test images: a) I1, b) I2, c) I3, d) I4, e) I5, f) I6, g) I7, h) I8, i) I9, and j) I10

5.3. Results

By applying the RC Algorithm (Section 3) to the Test images from the Test base (Fig. 3), without and with an inserted watermark, the following images have been obtained: a) Color Blind image (CB image), which is with colors as they are perceived by Deutan CVD people (Fig. 4), and b) Recolored image (RC image) intended for Deutan CVD people (Fig. 5). The binary watermark is shown in Fig. 6a. By applying the Block SVD Watermarking Algorithm (Section 5), the binary watermark has been inserted and extracted for the insertion factor $\alpha \in [0, 0.1]$, with a step of $\Delta\alpha = 0.005$. The extracted watermarks are shown in Fig. 6b ($\alpha = 0$), Fig. 6c ($\alpha = 0.025$), and Fig. 6d ($\alpha = 0.1$). In Fig. 7 shows Test image I6 (Fig. 3f) where the watermark is inserted with the insertion factor: a) $\alpha = 0$ (Fig. 7.a), b) $\alpha = 0.025$ (Fig. 7.b), and c) $\alpha = 0.1$ (Fig. 7c). In Fig. 8 RC I6 image is shown, where the watermark is inserted with the insertion factor: a) $\alpha = 0$ (Fig. 8a), b) $\alpha = 0.025$ (Fig. 8b), and c) $\alpha = 0.1$ (Fig. 8c). The objective measurements between the original and extracted watermarks are shown in: a) Fig. 9a (MSE), b) Fig. 9b (PSNR), c) Fig. 9c (NC), and d) Fig. 9d (SSIM). Objective measurements between the color components of: a) the Test image (RGB image) and Test image with inserted watermark, and b) the RC image and RC image with watermark are shown in: a) Fig. 10a (MSE), b) Fig. 10b (PSNR), c) Fig. 10c (NC), and d) Fig. 10d (SSIM), respectively.

The objective measurements between the original and the extracted watermark, after rotating of the RC image by angle $\theta = \{15^o, 30^o, 45^o, 60^o, 75^o\}$, are shown in a) Table 1 and b) Fig. 11. Fig. 12 shows the extracted watermarks, inserted with $\alpha_c = 0.025$, after rotation of the RC image for: a) $\theta = 15^o$ (Fig. 12a), b) $\theta = 30^o$ (Fig. 12b), c) $\theta = 45^o$ (Fig. 12c), d) $\theta = 60^o$ (Fig. 12d), and e) $\theta = 75^o$ (Fig. 12e). In Fig. 12f is shown the extracted watermark for $\alpha = 0.09$ and $\theta = 75^o$. The RC images, after rotation by angle $\theta = 75^o$ are shown in: a) Fig. 12g ($\alpha_c = 0.025$), and b) Fig. 12h ($\alpha = 0.09$). The objective measurements of the extracted watermark after scaling the RC image in the spatial domain, using the scaling factor $S_f = \{0.9, 0.8, 0.7, 0.6, 0.5\}$, are shown: a) tabular form (Table 2) and b) graphically (Fig. 13). The objective measurements of the extracted watermark after JPEG compression of the RC image, with quality factor $Q_{JPG} = \{100, 90, 80, 70, 60, 50\}$, are shown in Table 3. The objective measurements of the extracted watermark after TIFF, PGN and HDF compression of the RC image are mutually identical and, for the insertion factors $\alpha = \{0, 0.025, 0.05, 0.1\}$ are MSE = {1.3347, 0.1847, 0.0271, 0.0014}, PSNR = {1.3347, 7.3348, 15.6730, 28.5733}, NC = {0.5144, 0.7674, 0.9524, 0.9974} and SSIM = {0.0039, 0.3807, 0.7067, 0.9725}. Objective measurements for all compression algorithms are graphically shown in Fig. 14.

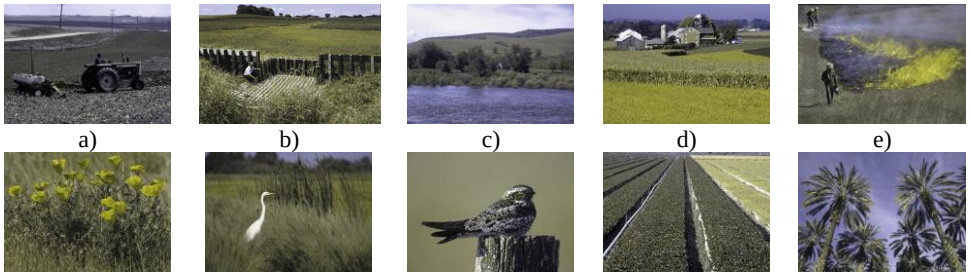

a) b) c) d) e)

f) g) h) i) j)

Fig. 4. CB images: a) I1, b) I2, c) I3, d) I4, e) I5, f) I6, g) I7, h) I8, i) I9, and j) I10

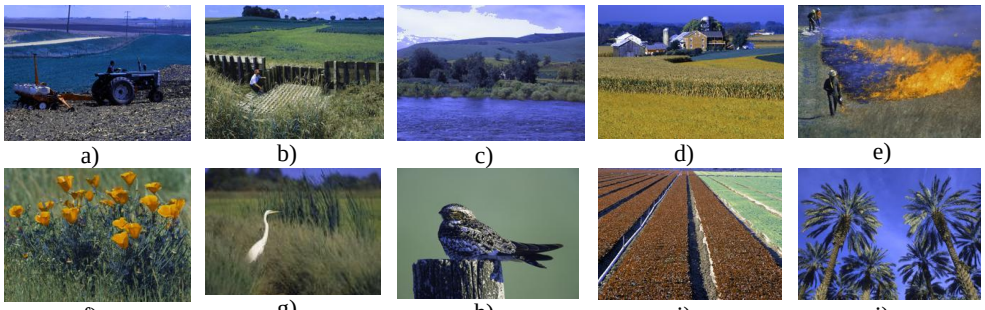

a) b) c) d) e)

f) g) h) i) j)

Fig. 5. RC image: a) I1, b) I2, c) I3, d) I4, e) I5, f) I6, g) I7, h) I8, i) I9, and j) I10

a) b) c) d)

Fig. 6. a) Binary watermark. Extracted watermark: b) $\alpha = 0$, c) $\alpha = 0.025$, and d) $\alpha = 0.1$

a) b) c)

Fig. 7. Test image I6 with inserted watermark with insertion factor: a) $\alpha = 0$, b) $\alpha = 0.025$, and c) $\alpha = 0.1$

a) b) c)

Fig. 8. RC image I6 with inserted watermark with insertion factor: a) α = 0, b) α = 0.25, and c) α = 0.1

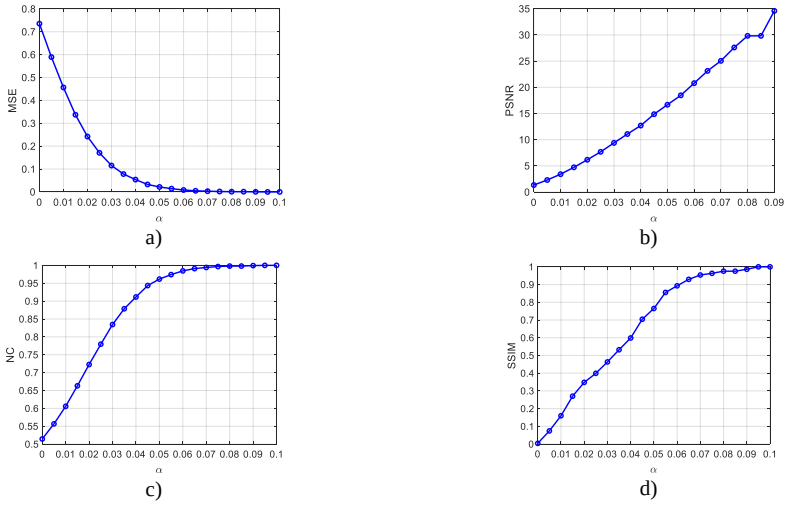

a) b) c) d)

Fig. 9. The objective measurements between the original and extracted watermarks: a) MSE, b) PSNR, c) NC, and d) SSIM

Table 1. The objective measurements between the original watermark and the extracted watermark after rotating the RC image by angle θ

MSE							
α	MSE_{wm}	θ (°)					$\overline{MSE_{RC\_\theta}}$
		15	30	45	60	75	
0	0.7354	0.7354	0.7354	0.7354	0.7354	0.7354	0.7354
0.025	0.1708	0.5517	0.5378	0.5264	0.5351	0.5517	0.5405
0.1	0	0.1326	0.1306	0.1257	0.1365	0.1257	0.1302
PSNR							
α	$PSNR_{wm}$	θ (°)					$\overline{PSNR_{RC\_\theta}}$
		15	30	45	60	75	
0	1.3347	1.3347	1.3347	1.3347	1.3347	1.3347	1.3347
0.025	7.6843	2.5827	2.6934	2.7869	2.7159	2.5827	2.6723
0.1	∞	8.7733	8.8420	9.0068	8.6500	9.0068	8.8558
NC							
α	NC_{wm}	θ (°)					$\overline{NC_{RC\_\theta}}$
		15	30	45	60	75	
0	0.5144	0.5144	0.5144	0.5144	0.5144	0.5144	0.5144
0.025	0.7795	0.5607	0.5671	0.5697	0.5666	0.5622	0.5653
0.1	1.0000	0.8115	0.8098	0.8161	0.8028	0.8178	0.8116
SSIM							
α	$SSIM_{wm}$	θ (°)					$\overline{SSIM_{RC\_\theta}}$
		15	30	45	60	75	
0	0.0039	0.0039	0.0039	0.0039	0	0.0039	0.0031
0.025	0.3991	0.0874	0.0942	0.0839	0.1003	0.0913	0.0914
0.1	1.0000	0.3975	0.3871	0.3950	0.3800	0.4009	0.3921

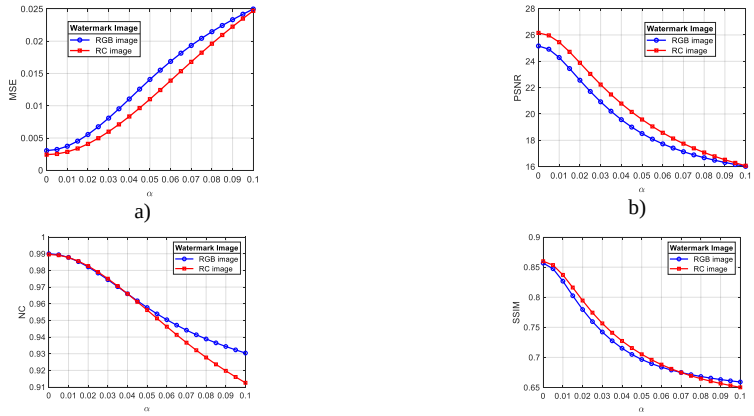

Fig. 10. The objective measurements between the Test image (RGB image) and Test image with inserted watermark, and RC image and RC image with inserted watermark: a) MSE, b) PSNR, c) NC, and d) SSIM

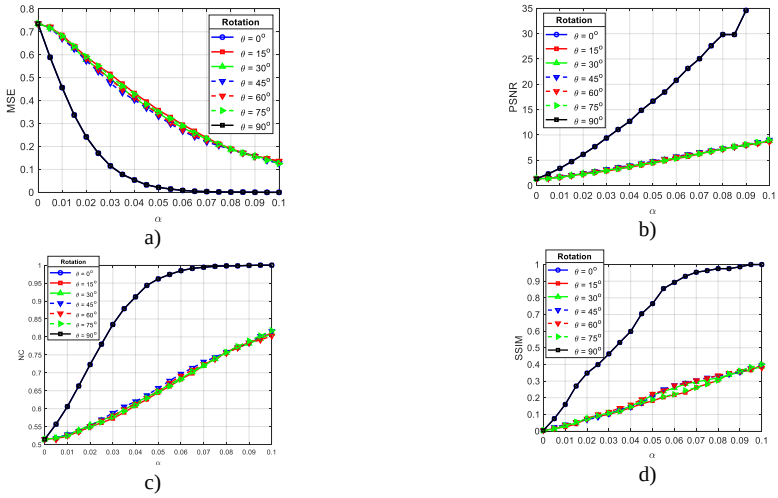

Fig. 11. The objective measurements between the original and the extracted watermark, after rotating of the RC image by angle θ: a) MSE, b) PSNR, c) NC, and d) SSIM

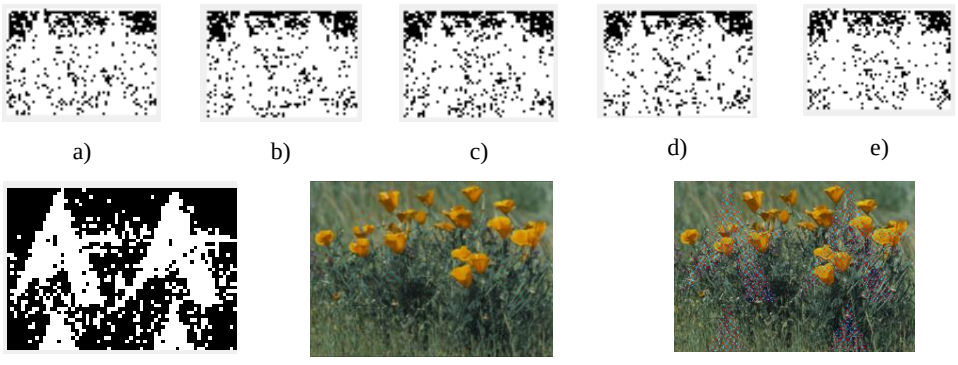

Fig. 12. The extracted watermarks (α_c = 0.025) after rotation for: a) θ = 15º, b) θ = 30º, c) θ = 45º, d) θ = 60º and e) θ = 75º. The RC image after rotation for θ = 75º for α_c = 0.025 (g), and α = 0.09 (h)

Table 2. The objective measurements of the extracted watermark after scaling the RC image by scaling factor S_f

MSE							
α	MSE_{wm}	S_f					$\overline{MSE_{S_f}}$
		0.9	0.8	0.7	0.6	0.5	
0	0.7354	0.7354	0.7354	0.7354	0.7354	0.7354	0.7354
0.025	0.1708	0.5510	0.5826	0.6073	0.6035	0.6069	0.5903
0.1	0	0.2069	0.2424	0.2955	0.3003	0.3149	0.2720
PSNR							
α	$PSNR_{wm}$	S_f					$\overline{PSNR_{S_f}}$
		0.9	0.8	0.7	0.6	0.5	
0	1.3347	1.3347	1.3347	1.3347	1.3347	1.3347	1.3347
0.025	7.6743	2.5882	2.3460	2.1660	2.1934	2.1685	2.2924
0.1	∞	6.8415	6.1554	5.2946	5.2238	5.0179	5.7066
NC							
α	NC_{wm}	S_f					$\overline{NC_{S_f}}$
		0.9	0.8	0.7	0.6	0.5	
0	0.5144	0.5144	0.5144	0.5144	0.5144	0.5144	0.5144
0.025	0.7795	0.5665	0.5538	0.5418	0.5425	0.5378	0.5485
0.1	1.0000	0.7439	0.7101	0.6651	0.6660	0.6426	0.6855
SSIM							
α	$SSIM_{wm}$	S_f					$\overline{SSIM_{S_f}}$
		0.9	0.8	0.7	0.6	0.5	
0	0.0039	0.0039	0	0.0039	0.0039	0.0039	0.0031
0.025	0.3991	0.0920	0.0629	0.0551	0.0499	0.0635	0.0647
0.1	1.0000	0.3407	0.3085	0.2247	0.2383	0.2181	0.2661

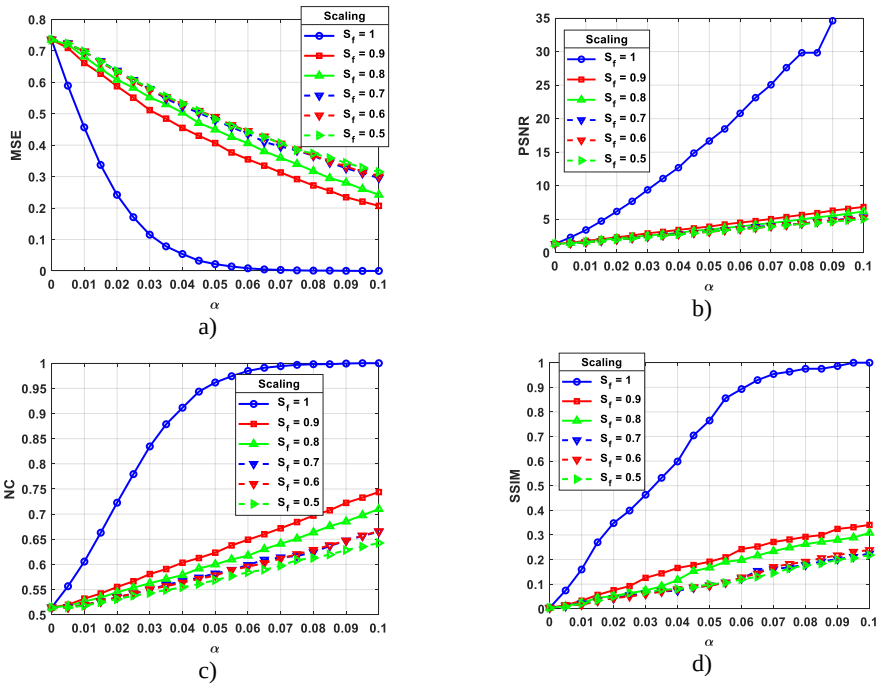

Fig. 13. The objective measurements between the original and extracted watermarks, after scaling of the RC image in the spatial domain, with the scaling factor S_f: a) MSE, b) PSNR, c) NC, and d) SSIM

Table 3. The objective measurements of the extracted watermark after JPEG compression, with quality factor Q_{JPG}

MSE							
α	Q_{JPG}						$\overline{MSE_{JPG}}$
	100	90	80	70	60	50	
0	0.7354	0.7354	0.7354	0.7354	0.7354	0.7354	0.7354
0.025	0.6056	0.6184	0.6229	0.6392	0.6424	0.6365	0.6275
0.1	0.2417	0.2510	0.2920	0.3201	0.3330	0.3378	0.2959
PSNR							
α	Q_{JPG}						$\overline{PSNR_{JPG}}$
	100	90	80	70	60	50	
0	1.3347	1.3347	1.3347	1.3347	1.3347	1.3347	1.3347
0.025	2.1785	2.0873	2.0557	1.9434	1.9222	1.9623	2.0249
0.1	6.1678	6.0025	5.3460	4.9466	4.7757	4.7128	5.3252
NC							
α	Q_{JPG}						$\overline{NC_{JPG}}$
	100	90	80	70	60	50	
0	0.5144	0.5144	0.5144	0.5144	0.5144	0.5144	0.5144
0.025	0.5258	0.5250	0.5256	0.5072	0.5068	0.5059	0.5161
0.1	0.7207	0.7131	0.6804	0.6546	0.6452	0.6364	0.6751
SSIM							
α	Q_{JPG}						$\overline{SSIM_{JPG}}$
	100	90	80	70	60	50	
0	0.0039	0.0039	0	0.0039	0.0039	0.0039	0.0032
0.025	0.0473	0.0448	0.0370	0.0437	0.0392	0.0352	0.0412
0.1	0.3447	0.3352	0.2975	0.2514	0.2279	0.2194	0.2793

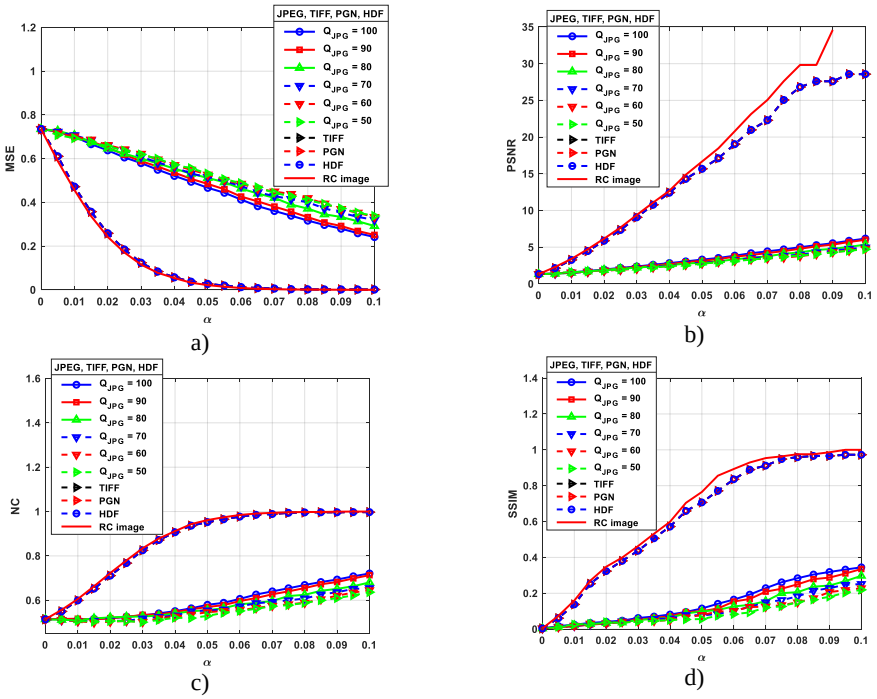

Fig. 14. The objective measurements between the original and extracted watermarks after JPEG, TIFF, PGN and HDF compression of the RC image: a) MSE, b) PSNR, c) NC, and d) SSIM

5.4. Analysis of results

Using the subjective method a visual inspection of the quality of: a) the Test image with an inserted watermark, b) the RC image with an inserted watermark, and c) the extracted watermark, has been performed. The mean value of the insertion factor α, at which the watermark is visible in the Test images (critical value of the insertion factor α_c), based on the subjective evaluations of the Test group, has been determined as $\alpha_c = \frac{1}{J \cdot K} \sum_{j=1}^{J} \sum_{k=1}^{K} \alpha_{c,j,k} = 0.025$, where $J = 10$ is the number of images in the Test base, and $K = 30$ is the number of members of the Test group. As an example, Fig. 7 shows the I6 Test image, for some values of the insertion factor: a) $\alpha = 0$ (Fig. 7a, no visual degradation), b) $\alpha = 0.025$ (Fig. 7b, threshold until the watermark is not visible in the image), and c) $\alpha = 0.1$ (Fig. 7c, large visual degradation, watermark visible in the image). Fig. 8 shows the I6 RC image, for: a) $\alpha = 0$ (Fig. 8a, no visual degradation), b) $\alpha = 0.025$ (Fig. 8b, threshold until the watermark is not visible in the image), and c) $\alpha = 0.1$ (Fig. 8c, large visual degradation, watermark visible in the image). Fig. 6a shows the watermark inserted into the I6 Test image. In addition, extracted watermarks are displayed for: a) $\alpha = 0$ (Fig. 6b, there is no watermark), b) $\alpha = 0.025$ (Fig. 6c, watermark quality is satisfactory for proving ownership of the image), and a) $\alpha = 0.1$ (Fig. 6d, high quality watermark). Subjective analysis shows two opposite tendencies that are observed with the increase of the insertion factor α: a) increasing visual degradation of the Test images and RC images, and b) reduces the visual degradation of the watermark.

The fact that, with an increase in the insertion factor, the visual quality of the extracted watermark increases, while the visual quality of the image decreases, can be clearly seen on the graphics, which represent objective measures, for a) extracted watermark (Fig. 9), and b) Test image and RC image (Fig. 10). On the graphics in Fig. 9, as shown by the subjective method, with increasing insertion factor α: a) MSE decreases (Fig. 9a), and b) PSNR (Fig. 9b), NC (Fig. 9c) and SSIM (Fig. 9d) are growing, which indicates an increase in the quality of the extracted WaterMark. The objective measures of degradation of the extracted, relative to the original watermark (Fig. 6a), obtained from the diagram of Fig. 9, for $\alpha_c = 0.025$, are: a) $MSE_{wm} = 0.1708$ (Fig. 9a), b) $PSNR_{wm} = 7.6743$ (Fig. 9b), and c) $NC_{wm} = 0.7795$ (Fig. 9c), and d) $SSIM_{wm} = 0.3991$ (Fig. 9c). The objective measures of degradation of the I6 Test image (RGB image) with an inserted watermark (Fig. 7), compared to the image without a watermark (Fig. 3f), are: a) $MSE_{RGB} = 0.0067$ (Fig. 10a), b) $PSNR_{RGB} = 21.7114$ (Fig. 10b), c) $NC_{RGB} = 0.9784$ (Fig. 10c), and c) $SSIM_{RGB} = 0.7595$ (Fig. 10d). The objective measures of degradation of the RC image with an inserted watermark (Fig. 8), compared to the RC image without a watermark (Fig. 5f), are: a) $MSE_{RC} = 0.0050$ (Fig. 10a), b) $PSNR_{RC} = 23.0401$ (Fig. 10b), c) $NC_{RC} = 0.9791$ (Fig. 10c), and d) $SSIM_{RC} = 0.7744$ (Fig. 10d). As an example of a drastically large insertion factor ($\alpha = 0.1$) in Fig. 6d shows the extracted watermark, which has an extremely high quality ($MSE_{wm} = 0$, $PSNR_{wm} = \infty$, $NC_{wm} = 1$, $SSIM_{wm} = 1$), and in Fig. 8c RC image that has extremely high visibility of the watermark ($MSE_{RC} = 0.0247$, $PSNR_{RC} = 16.0715$, $NC_{RC} = 0.9126$, $SSIM_{RC} = 0.6503$). Objective measures, as well as subjective measures, indicate that

increasing the insertion factor α affects the increase in the visual quality of the extracted watermark, as well as the decrease in the quality of the RC image.

The effects of rotation of the RC image on the quality of the extracted watermark are shown in Table 1, Fig. 11. and Fig. 12. Analyzing the data from Table 1 and the graphics representation in Fig. 11, it can be seen that the objective measurements differ insignificantly from each other for all rotation angles θ. The visual quality of the extracted watermarks, compared to the watermark of the unrotated RC image (Fig. 6c, $\alpha_c = 0.025$, $MSE_{wm} = 0.1708$) is largely degraded: a) $\theta = 15^o$ (Fig. 12a), b) $\theta = 30^o$ (Fig. 12b), c) $\theta = 45^o$ (Fig. 12c), d) $\theta = 60^o$ (Fig. 12d), and e) $\theta = 75^o$ (Fig. 12e). The rotation of the RC image has led to a decrease in the visual quality of the extracted watermark, shown by objective measures: a) $\overline{MSE_{RC\_\theta}}/MSE_{wm}$ = 0.5405/0.1708 = 3.16, b) $PSNR_{wm}/\overline{PSNR_{RC\_\theta}}$ = 7.6743/2.6723 = 2.87, c) $NC_{wm}/\overline{NC_{RC\_\theta}}$ = 0.7795/0.5653 = 1.38, and d) $SSIM_{wm}/\overline{SSIM_{RC\_\theta}}$ = 0.3991/0.0914 = 4.37 times, successively. Previous analyzes have shown that the visual quality of unrotated RC images, as well as the quality of extracted watermarks, is satisfactory for $\alpha_c = 0.025$ ($MSE_{wm} = 0.1708$). Analyzing the graph from Fig. 11a, it is concluded that, with the criterion of MSE equality ($MSE_{wm} = 0.1708$), satisfactory visual quality of the watermark is obtained for $\alpha_{ROT} = 0.09$ (Fig. 12f). In addition, a visual inspection of the quality of the RC image, which is rotated by the angle $\theta = 75^o$ (Fig. 12g) leads to the conclusion that the quality is satisfactory. However, this insertion factor leads to the degradation of the RC image (Fig. 12h), whose quality is reduced: a) $MSE_{RC\_\theta} = MSE_{RC}$ = 0.0102 / 0.0050 = 2.04, b) $PSNR_{RC}/PSNR_{RC\_\theta}$ = 23.0401 / 19.9256 = 1.15, c) NC_{RC} / NC_{RC_θ} = 0.9791 / 1.02 = 0.95, and d) $SSIM_{RC}/SSIM_{RC\_\theta}$ = 0.7744/0.6753 = 1.14 times, successively. Scaling of the RC image leads to a decrease in the quality of the extracted watermark (Table 2, Fig. 13): a) $\overline{MSE_{S_f}}/MSE_{wm}$ = 0.5903/0.1708 = 3.4561, b) $PSNR_{wm}/\overline{PSNR_{S_f}}$ = 7.6743/2.2924 = 3.3477, c) $NC_{wm}/\overline{NC_{S_f}}$ = 0.7795/0.5485 = 1.4211, and d) $SSIM_{wm}/\overline{SSIM_{S_f}}$ = 0.3991/0.0647 = 6.1685 times, successively. The MSE graph (Fig. 13.a) indicates the fact that in the tested range of inserting factors (α = 0 – 0.1) all MSE values are greater than $MSE_{wm} = 0.1708$. Therefore, it is concluded that, it is not possible by changing the insertion factor to achieve a satisfactory quality of the watermark, and that, therefore, scaling is very destructive. Applying the JPEG compression with reduced image quality Q_{JPG} = {90, 80, 70, 60, 50} of the RC image, the quality of the extracted watermark, compared to the watermark of the RC image without compression, is reduced: a) $\overline{MSE_{JPG}}/MSE_{wm}$ = 0.6275/0.1708 = 3.6739, b) $PSNR_{wm}/\overline{PSNR_{JPG}}$ = 7.6743/2.0249 = 3.7900, c) $NC_{wm}/\overline{NC_{JPG}}$ = 0.7795/0.5161 = 1.5104, and d) $SSIM_{wm}/\overline{SSIM_{JPG}}$ = 0.3991/0.0412 = 9.6869 times, successively. The MSE graph (Fig. 14.a) indicates the fact that, in the tested range of inserting factors ($\alpha \in [0, 0.1]$), all MSE values for Q_{JPG} = {90, 80, 70, 60, 50} are greater than $MSE_{wm} = 0.1708$. Therefore, it is concluded that, by changing the insertion factor, it is not possible to achieve a

satisfactory quality of the watermark, and that, therefore, JPEG compression is very destructive. In addition, by analyzing the objective measures shown graphically in Fig. 14, a great similarity between the measures for the watermark in: a) the RC image without compression, and b) the RC image after applying JPEG (for QJPG = 100), TIFF, PGN, and HDF compression algorithms, is observed. The use of the aforementioned algorithms for RC image compression leads to a decrease in the quality of the extracted watermark: a) MSE_{COMP}/MSE_{wm} = 0.1847/0.1708 = 1.0814, b) $PSNR_{wm}/PSNR_{COMP}$ = 7.6743/7.3348 = 1.0463, c) NC_{wm}/NC_{COMP} = 0.7795/0.7674 = 1.0158, d) $SSIM_{wm}/SSIM_{COMP}$ = 0.3991/0.3807 = 1.0483 times, successively.

The analysis of objective measures being carried out indicates the low robustness of the inserted watermark, which has been inserted using the Block SVD algorithm, in relation to spatial transformations (rotation, scaling) and compression algorithms that reduce image quality. The reason for the reduction of the robustness lies in the fact that one pixel of the watermark, after the SVD transformation is inserted into the $m \times m$ block of the image. In spatial transformations, and in order to maintain the grid, the intensity of each pixel of the RC image is interpolated to the nearest nodes of the grid. Therefore, the original values of the pixel intensity, and especially the pixel inserted watermark are irretrievably lost. This significantly reduces the robustness of the watermark.

6. Conclusion

The paper describes the image recoloring algorithm for Deutan CVD people. Then, the Block SVD algorithm for inserting a watermark into an RC image is shown. An experiment has been conducted in which the effect of inserting a watermark into an RC image on the degradation of its quality is analyzed. In addition, the effect of the visual degradation of the extracted watermark due to the application of the RC algorithm has been analyzed. The visual degradation of the watermark and RC image, by a subjective method, i.e., visual inspection is analyzed. Analysis of the results of objective measures (MSE, PSNR, NC and SSIM) shows that there is a degradation of the RC image with inserted watermark. In addition, it has been shown by objective measures that there is a degradation of the extracted watermark due to the application of the RC algorithm. Both methods, objective and subjective, unequivocally indicate the fact that with the increase in the insertion factor by α, the quality of the extracted watermark increases, while the quality of the RC image decreases. Visual inspection of the image (subjective method) has determined the threshold for watermark insertion factor, where the watermark and the RC image are of satisfactory quality ($\alpha_c = 0.02$).

The watermark, which is inserted by the Block SVD algorithm, enables proof of authorship over the RC image. Additionally, the analysis of the robustness of the watermark, which has been inserted into the RC image using the Block SVD algorithm has been performed. The robustness, in relation to attacks in the spatial domain (rotation, scaling) and transformation domain (JPEG, TIFF, PGN and HDF compression) is analyzed. A detailed analysis has pointed out the fact that with transformation algorithms whose compression is with a high quality factor ($Q > 90$),

the robustness of the watermark is high. However, with rotation and scaling attacks, as well as compression with a reduced quality factor ($Q < 90$), the robustness of the extracted watermark is very low, as indicated by objective quality measures. In addition visual inspection of the extracted watermark shows that it is not possible to recognize the watermark. Therefore, it is not possible to prove the authorship of the RC image.

References

1. Curcio, C., K. Sloan, R. Kalina, A. Hendrickson. Human Photoreceptor Topography. – J. Compar. Neurol., Vol. **292**, 1990, No 4, pp. 497-523.
2. Blake, R., R. Sekuler. Perception. New York, McGraw-Hill, 2006.
3. Zhenyang, Z., M. Toyoura, K. Go, K. Kashiwagi, I. Fujishiro, T. Wong, X. Mao. Personalized Image Recoloring for Color Vision Deficiency Compensation. – IEEE Transactions on Multimedia, Vol. **24**, 2021, pp. 1721-1734.
4. Sharpe, L., A. Stockman, H. Jagle, J. Nathans. Opsin Genes, Cone Photopigments, Color Vision, and Color Blindness. – In: K. Gegenfurtner, L. Sharpe, Eds. Book Color Vision: From Genes to Perception. Cambridge Univerity Press, 1999, pp. 3-51.
5. Milivojević, Z., B. Prlinčević, D. Kostić. Degradation Recoloring CVD Protan Image fom Blok SVD Watermark. – In: Proc. of 31th International Electrotechnical and Computer Science Conference ERK-2022, Portorož, Slovenia, 19-20 September 2022.
6. Nam, J., Y. Ro, Y. Huh, M. Kim. Visual Content Adaptation According to User Perception Characteristics. – IEEE Transactions on Multimedia, Vol. **7**, 2005, No 3, pp. 435-445.
7. Lin, H., L. Chen, M. Wang. Improving Discrimination in Color Vision Deficiency by Image Re-Coloring. – Sensors, Vol. **19**, 2019, No 10, pp. 22-50.
8. Hassan, M., R. Paramesran. Naturalness Preserving Image Recoloring Method for People with Red-Green Deficiency. – Signal Processing: Image Communication, Vol. **57**, 2017, pp. 126-133.
9. Milivojević, Z., M. Mladenović. Recoloring Ishimara Test Image for Protan CVD Persons. – International Journal the Power of Knowledge, Vol. **54**, 2022, No 3, pp. 447-452.
10. Hassan, M. Flexible Color Contrast Enhancement Method for Redgreen Deficiency. – Multidimensional Systems and Signal Processing, Vol. **30**, 2019, No 4, pp. 1975-1989.
11. Zhu, Z., M. Toyoura, K. Go, I. Fujishiro, K. Kashiwagi, X. Mao. Processing Images for Red-Green Dichromats Compensation via Naturalness and Information-Preservation Considered Recoloring. – The Visual Computer, Vol. **35**, 2019, No 6-8, pp. 1053–1066.
12. Milivojević, Z., B. Prlinčević, M. Cekić. Recoloring Ishihara Test Image for Deutan CVD Persons. – In: Proc. of 13th International Scientific Conference Science and Higher Education in Function of Sustainable Development – SED, 2023, Vrnjacka Banja, Serbia.
13. Pramoun, T., K. Thongkor, T. Amornraksa. Image Watermarking Against Color Blind Image Correction. Proceedings from Ubi-Media. – In: Proc. of 10th International Conference on Ubi-Media Computing and Workshops, 2017, pp. 1-6.
14. Pramoun, T., P. Supasirisun, T. Amornraksa. Digital Watermarking on Recolored Images for Protanopia. – In: Proc. of 15th International Conference on Electrical Engineering/Electronics, Computer, Telecommunications and Information Technology, 2018, pp. 62-65.
15. Crenshaw, C. Realtime Color Vision Deficiency Correction. U.S. Patent: 20140066196 A1, 2014.
16. Chang, C., Y. Hu, C. Lin. A Digital Watermarking Scheme Based on Singular Value Decomposition. – In: Proc. of 1st International Symposium ESCAPE, 2007, Hangzhou, pp. 82-93.
17. BSDS500 (Berkeley Segmentation Dataset).
https://www2.eecs.berkeley.edu/Research/Projects /CS/vision/bsds/

18. M i l i v o j e v i ć, Z., B. P r l i n č e v i ć. Degradation of the Recoloring Specific Degree Protan CVD Image From inserted Watermark. – In: Proc. of Information Teshnology – IT, 2023, Žabljak, Montenegro.
19. J e o n g, J., H. K i m, T. W a n g, Y. Y o o n, S. K o. An Efficient Re-Coloring Method with Information Preserving for the Color-Blind. – IEEE Transactions on Consumer Electronics, Vol. **57**, 2011, No 4, pp. 1953-1960.
20. M i l i v o j e v i ć, Z., B. P r l i n č e v i ć. Effect of Protan Recoloring Algorithm on Inserted Watermark in Presence of the Superimposed AWGN. – The Eurasia Proceedings of Science, Technology, Engineering & Mathematics (EPSTEM), 2022, pp. 116-124.
21. **https://www.pxfuel.com/en/desktop-wallpaper-ojhsd**
22. **https://www.pxfuel.com/en/desktop-wallpaper-jhehn**

Received: 31.08.2023; Second Version: 24.11.2023; Accepted: 12.01.2024